35th Annual International Conference of the IEEE EMBS
Osaka, Japan, 3 - 7 July, 2013

# Haptic perception of multi-joint hypertonia during simulated patient-therapist physical tele-interaction

D. Piovesan†, *IEEE Member*, A. Melendez-Calderon†*, *IEEE Member*, F.A. Mussa-Ivaldi

***Abstract*—A potential solution to provide individualized physical therapy in remote areas is tele-interaction via robotic devices. To maintain stability during tele-interaction, transmission delay-compensation algorithms bound the impedance between the patient and the therapist. This can compromise the haptic perception of the patient being assessed, which can in turn lead to a bad diagnosis or intervention. We investigated how the perception of the severity of hypertonia (a common condition after neurological disorders) varied by modifying the connection impedance on a physical simulator. We found that assessing hypetonia using a low impedance connection may result in an overestimation of mild impairments.**

***Key terms* –hypertonia, haptic perception, tele-rehabilitation**

## I. Introduction

NOWADAYS, about 50 million of USA citizens live in rural areas, and 75% of the USA surface is non-metropolitan [3]. Even in such advanced nations in the field of rehabilitation, specialized centers are often located in metropolitan areas, which often, are difficult to reach from remote locations. In the case of stroke, functional recovery has been linked to amount of therapeutic treatment and intensity of physical interactions during the rehabilitation regimen [4, 5]. Therefore, a logical step is to extend the interactive and personalized essence of current rehabilitation therapies to homes or local medical centers. To this end, tele-rehabilitation settings (e.g. [6-8]), where clinicians and patients can physically interact remotely via robotic devices (tele-interaction), can be of great help.

However, numerous problems may arise due to current network quality of service, such as jittering, time delays, etc. A way to mitigate the impact of transmission delays on stability is to allow the local and remote sites to interact with each other through a shared virtual environment [9, 10] which includes a simulated mechanical element. To maintain the stability of the system the impedance of such mechanical element is upper-bounded, which in turn compromises the haptic perception. In a nutshell, the practicality of a day-to-day tele-rehabilitation system is limited by the following: i) unless a complex exoskeleton is used on the remote site, the number of interaction points available for the therapist to physically manipulate the patient is very limited and ii) the perception of the patient's physical impairment via tele-interaction may be altered by the upper bound on the stiffness values that the delay-compensation algorithm imposes.

In this paper, we investigated how the severity of a simulated hypertonic arm is perceived by individuals when interacting via a single interaction port (e.g. arm manipulation by "holding" hands). We modeled a patient's arm characterized by different levels of hypertonia and connected this virtual arm and the operator via a virtual spring-damper using a two degrees-of-freedom robotic manipulandum [11]. We investigated how the perception of the severity of hypertonia varied by modifying the connection impedance. This study systematically analyzes the perception of both position and velocity-dependent stiffness of a multi-joint system, analogous to a hypertonic arm. This will allow parameterizing such interaction with mathematical models associating the subjective experience of the therapist with objective values of arm mechanics.

## II. Methods

Ten right-handed subjects (age 25 to 35 years) naïve to the experimental conditions participated in the study. Subjects gave informed consent prior participation. Experiments were approved by the Rehabilitation Institute of Chicago's Institutional Review Board.

### A. Apparatus

Subjects seated in front of a two degrees-of-freedom robotic manipulandum and interacted with a physical model of an arm by holding the robot's end effector (Figure 1). The model was implemented in Simulink and was executed in real-time using xPC Target at a rate of 1 kHz.

Both the subjects' hand and the robotic arm were covered by an opaque horizontal screen, on which the image of the rendered virtual arm was projected. The image of a 35 cm diameter circle was shown centered at the virtual arm endpoint and represented most of the virtual arm workspace. Before the beginning of each trial, subjects saw the static image of the arm while a white dot moved synchronously with the position of the subject hand. In order to activate the trial, subjects needed to bring the white dot to the depicted virtual hand. Thus, the white dots would turn green, the virtual arm would start moving as a function of the subject

D. Piovesan†, A. Melendez-Calderon†, and F.A. Mussa Ivaldi are with the Sensory Motor Performance Program at the Rehabilitation Institute of Chicago, Illinois, U.S.A. (e-mail: [alejandro.melendez, d-piovesan]@northwestern.edu). *Asterisk indicates corresponding author.* † *indicates equal contribution*. This work was partially supported by NNINDS grant 2R01NS035673; AMC was supported by the Coolidge Postdoctoral fellowship

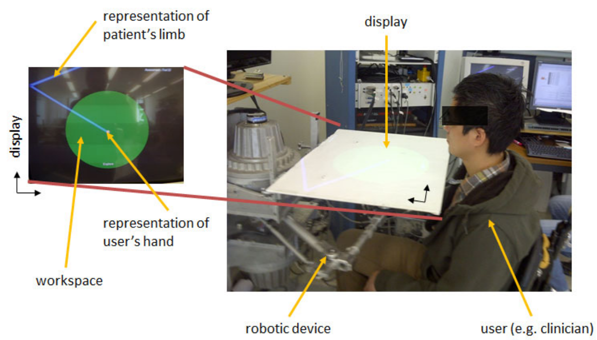


Figure 1 – Subject interacting with a simulated hypertonic arm.

hand position and the force field was rendered.

## B. *Experimental protocol*

The experiment was divided in two consecutive phases: *i)* familiarization and *ii)* assessment. During *familiarization*, the participants interacted with the virtual arms encompassing 3 level of hypertonia: *very mild, mild,* and *moderate* for 10s. Subjects' and virtual arm were connected via a virtual spring-damper system with stiffness of 1625 [N/m], critically damped. All subjects interacted sequentially with each condition in blocks of 10s for five times (5 presentations x 3 conditions = 15 familiarization trials). During familiarization, a legend appeared on the top right corner of the screen indicating the condition that the subject was experiencing.

Subjects were free to interact with those three conditions as they wished in order to familiarize with the different haptic sensations produced by the hypertonic arm. During assessment, subjects were randomly presented with the aforementioned hypertonic virtual arms where the stiffness of the virtual spring was either 1050, 1625, or 2200 [N/m] (critically damped). Their task was to identify the level of hypertonia of the virtual arm. Subjects were presented each condition twelve times in blocks of 5s (3 virtual objects x 3 levels of severity x 12 presentations = 108 trials). The only feedback given to the subjects was the configuration of the virtual arm and the rendered force at the end effector. After manipulation, subjects were required to select one of three options: *very mild*, *mild* or *moderate*.

## C. *Neuro-mechanical model of the human arm*

The dynamics of the virtual arm moving in a horizontal plane while interacting with the environment were modeled as:

$$\begin{aligned} H(q)\ddot{q} + C\left(q,\dot{q}\right)\dot{q} &= J_q\left(q\right)^T \cdot F_{\text{external}} \\ &\quad - J_\lambda^T \cdot \left(\Phi\left(\lambda, u(\dot{\lambda})\right) + \Psi\left(\lambda\right)\right) \end{aligned} \tag{1}$$

$H\left(q\right)$ is the arm inertia matrix of a double pendulum system , $q$ denote the vector of shoulder and elbow joint angles [rad], $C\left(q,\dot{q}\right)\dot{q}$ is the term corresponding to Coriolis and centripetal forces, $J_q\left(q\right)$ is the Jacobian matrix transforming endpoint force into joint torque.

We assumed the Jacobian matrix transforming muscle tension into joint torque, $J_\lambda$ to be independent of the muscle lengths $\lambda$ [2]. This term contains the muscle moment arms $\rho$ at any particular position which for simplicity can be considered constant with values falling on reported anthropometric data in the literature, thus:

$$J_\lambda = \begin{pmatrix} -\rho_{sf} & \rho_{se} & 0 & 0 & -\rho_{bf_1} & \rho_{be_1} \\ 0 & 0 & -\rho_{ef} & \rho_{ee} & -\rho_{bf_2} & \rho_{be_2} \end{pmatrix}^T \tag{2}$$

The sub-indexes correspond to *sf*, shoulder adductors (Deltoid anterior, Coracobrachialis, Pectoralis major clav.); *se,* the shoulder abductors (Deltoid posterior); *ef,* elbow flexors (Biceps long, Brachialis, Brachioradialis); *ee,* elbow extensors (Triceps lateral, Anconeus); *bf,* bi-articular flexors (Biceps short); and *be,* bi-articular extensors (Triceps long) muscle groups. Simulation-specific parameters are reported in Table I.

The force of each muscle group was modeled as a linear combination of an active motor command, $u$ and passive components associated with intrinsic rigidity of the muscles and connective tissue. The force produced by each muscle in response to the motor command $u$ is:

$$\begin{aligned} \Phi(\lambda, u(\dot{\lambda})) &= \begin{pmatrix} \varphi_{sf} & \varphi_{se} & \varphi_{ef} & \varphi_{ee} & \varphi_{bf} & \varphi_{be} \end{pmatrix}^T \\ \varphi_i &= \max\begin{pmatrix} 0, \\ \alpha_i u(\dot{\lambda}_i)\cdot\Gamma\cdot e^{-\left(\frac{\Gamma}{0.5u^2(\dot{\lambda}_i)+0.1}\right)^2} \end{pmatrix} \\ \Gamma &= \left(\frac{\lambda_i}{\lambda_{\max,i}} - \frac{\lambda_{rest,i}}{\lambda_{\max,i}}\left(1-u(\dot{\lambda}_i)\right)\right) \end{aligned} \tag{3}$$

The term $\tau$ corresponds to the muscle stiffness, and $u(\dot{\lambda})$ to an active motor command that depends on the muscle stretch velocity and is defined as:

TABLE I - INERTIAL AND GEOMETRICAL PARAMETERS

| Symbol | Denomination | Value |
|---|---|---|
| $m_{subject}$ | Subject mass* | 75 [kg ] |
| $l_1$, $l_2$ | Upper and lower arm length* | 0.31,0.35 [m] |
| $r_1$, $r_2$ | Upper and lower arm center of mass* | 0.135, 0.150 [m] |
| $m_1$, $m_2$ | Upper and lower arm mass* | 2.1, 1.2 [kg] |
| $I_1$, $I_2$ | Upper and lower arm moment of inertia about the proximal joint* | 0.0593, 0.0407 [kg m$^2$] |
| $\rho_{sf}$, $\rho_{se}$ | Shoulder adductors and abductors moment arm** | 0.03, 0.03 [m] |
| $\rho_{ef}$, $\rho_{ee}$ | Elbow flexors and extensors moment arm** | 0.021, 0.021 [m] |
| $\rho_{bf1}$, $\rho_{bf2}$, $\rho_{be1}$, $\rho_{be2}$ | Biarticular flexors and extensors moment arm** | 0.044, 0.044, 0.0338, 0.0338 [m] |

* from equations proposed in [1]; ** as defined in [2]

$$u(\dot{\lambda}_i) = \beta_i \min\left(1, \max\left(0, \frac{\dot{\lambda}_i}{\dot{\lambda}_{\max,i}}\right)\right) \quad | \quad \beta_i \in [0,1] \tag{4}$$

where $\beta$ corresponds to a "stretch reflex gain". The variables $\lambda_{rest,i}$, $\lambda_{\max,i}$, and $\dot{\lambda}_{\max,i}$ correspond to the length of the $i^{th}$ muscle group at rest, its maximum length and maximum rate of length change, respectively. The maximum rate of length change was calculated as the one obtained by moving the end point of virtual arm along the circle of 35cm in diameter at a frequency of 2Hz.

The force produced by the intrinsic rigidity of the muscles and connective tissue is function of the muscle length and is defined as:

$$\Psi(\lambda) = (\psi_{sf} \quad \psi_{se} \quad \psi_{ef} \quad \psi_{ee} \quad \psi_{bf} \quad \psi_{be})^T$$
$$\psi_i = \max\begin{pmatrix} 0, \\ K_{m,i}\left(\lambda_i - \lambda_{rest,i}\right)e^{-\left(\lambda_i - \lambda_{rest,i}\right)^2} \end{pmatrix} \tag{5}$$

The term $\Psi(\lambda)$ can be multiplied by a generalized logistic function to avoid sharp discontinuities when adding both passive and active components in eq. (1). The term $\lambda$ and $K_m$ represent the muscle length and muscle rigidity respectively.

### D. Selection of rigidity boundary parameters

Measurements of joint rigidity during passive movements are available in the literature for both stroke survivors and unimpaired individuals [12, 13]. Based on such data, we assumed the average joint passive stiffness of unimpaired individuals as the *lower boundary* of joint rigidity, namely: $K_q = \begin{pmatrix} 2 & 0.5 \\ 0.5 & 1 \end{pmatrix} [N \cdot m / rad]$. The *upper boundary* of joint rigidity was set as $K_q = \begin{pmatrix} 14 & 3 \\ 3 & 8 \end{pmatrix} [N \cdot m / rad]$, this value corresponds to the passive stiffness recorded on stroke survivors with Modified Ashworth Score (MAS) equal to 4 [14, 15].

### E. Simulating hypertonic-like forces

Among the numerous factors that characterize hypertonia we are interested in verifying the participants' ability to discriminate forces produced by increased muscle rigidity and the nonlinear phenomena associated with velocity dependent stiffness. We assumed that hypertonic-like forces could be achieved by increasing both the muscle stiffness $\alpha$ and intrinsic rigidity $K_m$ in eqs. (3) and (5). Our goal was to simulate several degrees of hypertonia that could be identified by individuals via their own proprioceptive feedback. The just noticeable difference (JND), or Weber fraction, is an important index representing the sensitivity of the subject to stiffness stimuli. Stiffness JND is defined as the ratio between the perceived difference in stiffness about a specific stiffness level and the stiffness level itself normalized to 100 (i.e. $JND = \Delta K / K \cdot 100$). In general $\Delta K$ is the stimulus difference between the first and the third quartile of a stiffness distribution. Different stiffness JND have been obtained empirically, depending on the experimental protocol used. For palpation with a fixed displacement, the value of stiffness JND is around 8% [16]. For free exploration, the JND is much higher and can be up to 67% [17]. Since the rigidity discrimination in the clinical setting is performed with a free movement we imposed as a first approximation a stiffness JND=60% which corresponds to a Weber fraction of 0.6. Knowing the Weber fraction of stiffness allowed us to set adjacent stiffness levels thus, segmenting the whole range of rigidity between the two aforementioned boundary conditions using five possible levels. The ratio between the stiffness at different levels for the specific muscle group *i* was set so that:

$$\frac{K_{m,i}^{level}}{K_{m,i}^{level+1}} \in \left[\frac{3}{5}, \frac{5}{8}, \frac{8}{13}, \frac{13}{21}\right] | \; level = 0..4 \Rightarrow$$
$$\Rightarrow K_{m,i}^{level} = \kappa_{\text{level}} \, K_{\text{nominal},i} \; | \; \kappa = \{3,5,8,13,21\} \tag{6}$$

thus following a Fibonacci sequence that approximate a 0.6 Weber fraction. Notice that also the MAS encompasses five ordinal levels (i.e. 0,1/1+,2,3,4) analogous to five levels of severity – "*normal"*, *very mild*, *mild*, *moderate* and *severe*. A score of 0 represents a "normal" joint stiffness and a score of 4 corresponds to a very rigid joint (i.e. very hard to move). In addition, it is important to notice that given the linearity of the Jacobian transformation between muscles', joints' and Cartesian space, multiplying the muscle stiffness matrix by $\kappa$ will increase rigidity in all the other three spaces in the same proportion. The values for the nominal muscle stiffness were chosen as:

$$K_{\text{nominal}} = (k_{sf} \quad k_{se} \quad k_{ef} \quad k_{ee} \quad k_{bf} \quad k_{be}) = $$
$$(540 \quad 540 \quad 600 \quad 600 \quad 100 \quad 100) \quad [N/m] \tag{7}$$

The ratio between muscle stiffness and rigidity of the connective tissue has been reported to vary between 1:1 and 1:10 [18-21]. We assumed the intrinsic muscle stiffness $\alpha$ to be $K_m^{level}/4$. Hence, by varying $K_m^{level}$ according to eq. (8) would automatically produce an increase in the active force $\Phi$ following a Weber law.

TABLE II - JOINT AND CARTESIAN STIFFNESS WHEN ALL MUSCLE GROUPS ARE IMPAIRED

| Level of severity | $\upsilon$ | $\kappa$ | $K_q \mid \dot{\lambda} = 0$ $[\text{N} \cdot \text{m/rad}]$ | $K_x \mid \dot{\lambda} = 0$ $[\text{N/m}]$ |
|---|---|---|---|---|
| **Very mild** | **0.25** | **5** | $\begin{pmatrix} 3.39 & 0.78 \\ 0.78 & 1.96 \end{pmatrix}$ | $\begin{pmatrix} 39.14 & -17.76 \\ -17.76 & 29.54 \end{pmatrix}$ |
| **Mild** | **0.5** | **8** | $\begin{pmatrix} 5.43 & 1.26 \\ 1.26 & 3.15 \end{pmatrix}$ | $\begin{pmatrix} 62.62 & -28.42 \\ -28.42 & 47.27 \end{pmatrix}$ |
| **Moderate** | **0.75** | **13** | $\begin{pmatrix} 8.83 & 2.05 \\ 2.05 & 5.15 \end{pmatrix}$ | $\begin{pmatrix} 101.76 & -46.18 \\ -46.18 & 76.82 \end{pmatrix}$ |

We imposed a concurrent linear variation of $\upsilon$ from 0 to 1 in eq. (4) in intervals so to obtain five equally spaced levels of reflex gains which can be associated to the five levels of severity of our task. To render the different hypertonic conditions in our experiment, the hypertonic gains (i.e. $\upsilon$ and $\varrho$ in Eqs. (4) and (6)) were applied to all the muscle groups. Furthermore, to simplify the task we tested only 3 levels of impairment (very mild, mild, and moderate) as shown in Table II.

### A. *Connection between subject and the human arm model*

Participants interacted with the arm model via a two-way connection implemented by a simple spring-damper model.

Given the end-point inertial matrix of the virtual arm, $M_{hand} = \begin{bmatrix} 2.76 & -1.78 \\ -1.78 & 1.98 \end{bmatrix} [kg]$, calculated in the center of the workspace, the maximum mass eigenvalue is equal to 4.2[kg]. Moving the virtual arm via the connection stiffness can give rise to a "slingshot effect", where a single overshoot in response to a step response generates a rebound that is often misinterpreted as the effect of the velocity dependent stiffness. Indeed, this phenomenon can occur even if the connection is critically dampened. To avoid this effect we empirically tuned the connection stiffness and found that the perception of the rebound was negligible for a stiffness of 1050 [N/m], which was assumed as the lower bound of the stiffness connection. This imposes a cut off frequency proper of the connection (i.e. a mechanical second order filter) to2.5 [Hz]. To this end the stiffness values of the connection were equal to 1050, 1625 and 2200 [N/m].

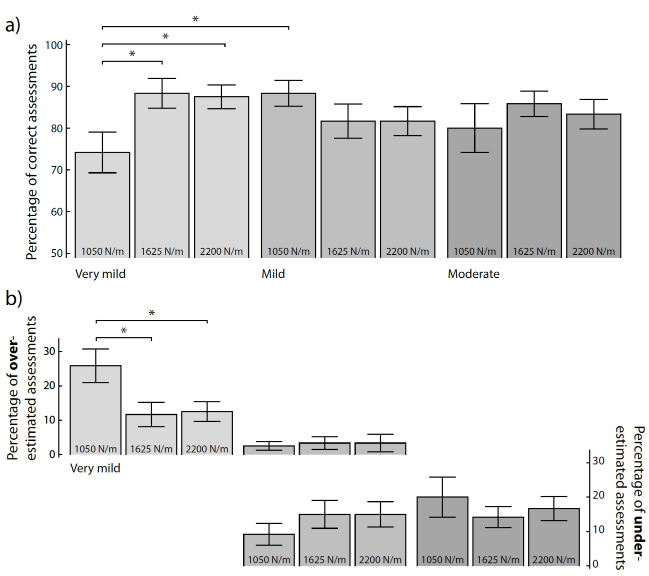


Figure 2 – Mean and standard error (n=10) of the percentage of (a) correctly assessed trials and (b) over- and under-estimated trials at different levels of hypertonic severity (very mild, mild and moderate) when interacting with the arm model with different connection impedances (1050, 1625 and 2200 N/m).

## III. Results

A repeated measures ANOVA with *subjects* as random factor was performed. There was no significant effect of *connection* impedance (F=1.730, p=0.205) or level of *severity* (F=0.028, p=0.971). However, there was a significant interaction effect between connection and severity (F=3.630, $p<0.05$) suggesting that the perception of the hypertonic condition may be affected by the connection impedance. Figure 2 shows the percentage of correctly assessed trials and the percentage of trials in which the level of severity was either over or under estimated. The data suggests subjects may perceive a higher stiffness when the severity is mild and the connection impedance is low (i.e. 1050 N/m in our experiment).

## IV. Conclusion

We investigated the capability of naïve subject to assess an absolute value of velocity dependent non-linear stiffness, which is physiologically compatible with the hypertonic behavior of two degrees of freedom upper limbs. Most of the experiments that have investigated the precision of stiffness perception focused on non-biological stiffness which generates a linear position dependent force field [22-24]. Those studies that did investigate physiologically compatible stiffness, analyzed single degrees of freedom movements, in order to correlate human perception with existing clinical scales [25-30].

The aim of this study was to look at the relationship between physical and perceived biological stiffness, at different magnitudes and with different contact impedances, to obtain more insight into how delay-compensating algorithms may affect perception. It is important to highlight that when therapist make an assessment of hypertonia, they can make a direct comparison between the unimpaired and impaired arm, but in the end they need to provide a score that is on an absolute scale. Secondly, we provide preliminary evidence that assessing hypertonic-like limbs via a single haptic port is feasible, even though, a direct comparison with clinical scale is not directly possible, as the latter are based on single joint assessments. This has a direct impact on the design of assessment protocols to be used during tele-rehabilitation treatments, where single haptic ports are usually the only option. We also demonstrated that by maintaining the stiffness of the shared object to a moderate level, the perception of biologically compatible stiffness is not undermined.

We are using similar methodologies to study how naïve subjects and expert therapists identify the nature and severity of hypertonic impairments [31, 32].

## V. Acknowledgments

We thank Prof. James Patton for his valuable suggestions.

## VI. References


[1] D. A. Winter, *Biomechanics and motor control of human movement*, 3rd ed.: John Wiley & Sons, 2004.

[2] D. W. Franklin, E. Burdet, P. T. Keng, R. Osu, C. M. Chew, T. E. Milner, *et al.*, "CNS learns stable, accurate, and efficient movements using a simple algorithm," *Journal of Neuroscience,* vol. 28, pp. 11165-11173, 2008.

[3] K. Johnson, "Reports on Rural America: Demographic Trends in Rural and Small Town America," Carsey Institute; Annie E. Casey Foundation; W.K. Kellogg Foundation, 2006.

[4] G. Kwakkel, R. C. Wagenaar, T. W. Koelman, G. J. Lankhorst, and J. C. Koetsier, "Effects of intensity of rehabilitation after stroke. A research synthesis," *Stroke,* vol. 28, pp. 1550-6, Aug 1997.

[5] P. Langhorne, R. Wagenaar, and C. Partridge, "Physiotherapy after stroke: more is better?," *Physiother Res Int,* vol. 1, pp. 75-88, 1996.

[6] H. Sugarman, E. Dayan, A. Weisel-Eichler, and J. Tiran, "The Jerusalem TeleRehabilitation System, a new low-cost, haptic rehabilitation approach," *Cyberpsychology & behavior,* vol. 9, pp. 178-82, 2006.

[7] J. Tang, C. Carignan, and S. Gattewar, "Virtual Environment for Robotic Tele-Rehabilitation," *9th International Conference on Rehabilitation Robotics, 2005. ICORR 2005.,* pp. 365-370, 2005.

[8] X. Wang and J. Li, "Feasibility of a Tele-rehabilitation System with Corrective-Force," *2011 International Conference on Virtual Reality and Visualization,* pp. 259-262, 2011.

[9] J.-P. Kim and J. Ryu, "Robustly Stable Haptic Interaction Control using an Energy-bounding Algorithm," *Int. J. Rob. Res.,* vol. 29, pp. 666-679, 2010.

[10] C. R. Carignan and P. A. Olsson, "Cooperative control of virtual objects over the Internet using force-reflecting master arms," in *Robotics and Automation, 2004. Proceedings. ICRA '04. 2004 IEEE International Conference on*, 2004, pp. 1221-1226 Vol.2.

[11] A. Melendez-Calderon*, D. Piovesan*, F. A. Mussa-Ivaldi, and J. L. Patton, "Haptic simulator of abnormal biomechanics during patient-clinician interaction," in *Proceedings of the IEEE International Conference on Robotics and Automation (ICRA) Workshop on Developments of Simulation Tools for Robotics & Biomechanics*, Karlsruhe, Germany, 2013.

[12] R. L. Watts, A. W. Wiegner, and R. R. Young, "Elastic properties of muscles measured at the elbow in man: II. Patients with parkinsonian rigidity," *J Neurol Neurosurg Psychiatry,* vol. 49, pp. 1177-81, Oct 1986.

[13] Z. Li-Qun, P. Hyung-Soon, and R. Yupeng, "Shoulder, elbow and wrist stiffness in passive movement and their independent control in voluntary movement post stroke," in *Rehabilitation Robotics, 2009. ICORR 2009. IEEE International Conference on*, 2009, pp. 805-811.

[14] J. D. Given, J. P. Dewald, and W. Z. Rymer, "Joint dependent passive stiffness in paretic and contralateral limbs of spastic patients with hemiparetic stroke," *Journal of Neurology, Neurosurgery & Psychiatry,* vol. 59, pp. 271-279, September 1, 1995 1995.

[15] Piovesan D., Morasso P., Giannoni P., and Casadio M., "Arm Stiffness During Assisted Movement After Stroke: The Influence Of Visual Feedback And Training," *IEEE Transactions on Neural Systems and Rehabilitation Engineering.,* vol. 10.1109/TNSRE.2012.2226915, 2012.

[16] H. Z. Tan, N. I. Durlach, G. L. Beauregard, and S. M.A., "Manual discrimination of compliance using active pinch grasp: The roles of force and work cues.," *Perception & Psychophysics,* vol. 57, pp. 495–510, 1995.

[17] S. Youngung and S. McMains, "Evaluation of drawing on 3D surfaces with haptics," *Computer Graphics and Applications, IEEE,* vol. 24, pp. 40-50, 2004.

[18] Piovesan D., Pierobon A., and Mussa-Ivaldi F.A. (2012, Third-Order Muscle Models: The Role of Oscillatory Behavior in Force Control. . *International Mechanical Engineering Congress & Exposition ASME -IMECE,* .

[19] C. S. Cook and M. McDonagh, "Measurement of muscle and tendon stiffness in man," *european journal of applied physiology,* vol. 72, pp. 380-382, 1996.

[20] I. D. Loram, M. Lakie, I. Di Giulio, and C. N. Maganaris, "The consequences of short-range stiffness and fluctuating muscle activity for proprioception of postural joint rotations: the relevance to human standing," *Journal of Neurophysiology,* vol. 102, pp. 460-74, 2009.

[21] T. a. L. Wren, "A computational model for the adaptation of muscle and tendon length to average muscle length and minimum tendon strain," *Journal of Biomechanics,* vol. 36, pp. 1117-1124, 2003.

[22] B. R. Brewer and M. Fagan, "Perceptual limits for a robotic rehabilitation environment using visual feedback distortion," *IEEE transactions on neural systems and rehabilitation engineering,* pp. 1-11, 2005.

[23] N. Forrest and S. Baillie, "A comparative study of haptic stiffness identification by veterinarians and students," *IEEE TRANSACTIONS ON HAPTICS,* vol. 4, pp. 78-87, 2011.

[24] L. Nicholson, R. Adams, and C. Maher, "Reliability of a discrimination measure for judgements of non-biological stiffness," *Manual Therapy,* vol. 2, pp. 150-156, 1997.

[25] D. I. Grow, M. Wu, M. J. Locastro, S. K. Arora, A. J. Bastian, and A. M. Okamura, "Haptic Simulation of Elbow Joint Spasticity," *2008 Symposium on Haptic Interfaces for Virtual Environment and Teleoperator Systems,* pp. 475-476, 2008.

[26] T. Kikuchi and K. Oda, "Preliminary experimental evaluation using a leg-shaped haptic simulator to quantify the diagnosing technique of ankle clonus," *2010 IEEE/ASME International Conference on Advanced Intelligent Mechatronics,* pp. 1317-1322, 2010.

[27] T. Kikuchi and K. Oda, "Dynamics simulation of a neuromuscular model of ankle clonus for neurophysiological education by a leg-shaped haptic simulator," *2010 IEEE/SICE International Symposium on System Integration,* pp. 329-334, 2010.

[28] T. Kikuchi, K. Oda, S. Yamaguchi, and J. Furusho, "Leg-robot with MR clutch to realize virtual spastic movements," *Journal of Physics: Conference Series,* vol. 149, pp. 012060-012060, 2009.

[29] H.-S. Park, J. Kim, and D. L. Damiano, "Haptic recreation of elbow spasticity," *IEEE International Conference on Rehabilitation Robotics* vol. 2011, pp. 5975462-5975462, 2011.

[30] H.-S. Park, J. Kim, and D. L. Damiano, "Development of a Haptic Elbow Spasticity Simulator (HESS) for improving accuracy and reliability of clinical assessment of spasticity," *IEEE transactions on neural systems and rehabilitation engineering,* vol. 20, pp. 361-70, 2012.

[31] A. Melendez-Calderon*, D. Piovesan*, and F. A. Mussa-Ivaldi, "Therapist discrimination of impaired muscle groups in simulated multi-joint hypertonia," in *13th Intern. Conf. on Rehab. Robotics IEEE ICORR*, 2013.

[32] D. Piovesan*, A. Melendez-Calderon*, and F. A. Mussa-Ivaldi, "Haptic discrimination of multijoint dystonia and spasticity in the assessment of hypertonia. ," in *13th Intern. Conf. on Rehab. Robotics IEEE ICORR*, 2013.